Triangular spectral phase tailoring for the generation of high-quality picosecond pulse trains

Ugo Andral, Christophe Finot

Triangular spectral phase tailoring for the generation of high-quality picosecond pulse trains

Ugo Andral and Christophe Finot *
Laboratoire Interdisciplinaire CARNOT de Bourgogne, UMR 6303 CNRS-Université de Bourgogne Franche-Comté, Dijon, France

ABSTRACT

The generation of high quality pulse trains at repetition rates of several tens of GHz remains a crucial step for optical telecommunications, optical sampling or component testing applications. Unfortunately, the current bandwidth limitations of optoelectronic devices do not allow the direct generation of well-defined optical pulse trains with low duty cycles. A linear solution is based on a direct temporal phase modulation that is then converted into an intensity modulation thanks to a dispersive element. However, this approach suffers from a limited extinction ratio or from the presence of detrimental temporal sidelobes. We introduce here theoretically and experimentally an alternative scheme where the quadratic spectral phase is replaced by a triangular one. With such a specific phase processing, Fourier-transform limited structures are obtained, with properties that may present some similarities with Akhmediev breathers at the point of maximum focusing. Experimental validation carried at repetition rates between 10 and 40 GHz confirm that high-quality close-to-Gaussian pulse trains can be achieved with an excellent extinction ratio and with a duty cycle below 1/4, in full agreement with our numerical simulations and analytical predictions. The resulting pulse train exhibits a remarkable stability. The proposed approach can be extended to process several wavelengths simultaneously as demonstrated by the experimental generation of 4 interleaved pulse trains in the conventional C-band. The versatility of the proposed scheme also enables the generation of pulse trains with varying pulse-to-pulse delays or durations.

Keywords: Phase modulation, ultrashort pulse trains, optical shaping, high-repetition rates sources.

1. INTRODUCTION

The generation of high quality pulse trains at repetition rates of several tens of GHz remains a crucial step for optical telecommunications, optical sampling or component testing applications. Unfortunately, the current bandwidth limitations of optoelectronic devices do not allow the direct generation of well-defined optical pulse trains with low duty cycles. Several cavity-free nonlinear operation techniques have been suggested benefiting from the nonlinearity of optical fibers to reshape a sinusoidal intensity modulation [1-3].

An alternative linear solution is based on a direct temporal phase modulation that is then converted into an intensity modulation. A well-known approach is based on a dispersive element that imprints a spectral quadratic phase. Picosecond pulses at repetition rates of several tens of GHz have been successfully demonstrated [4, 5] and tested for optical sampling [6]. However, this approach suffers from a limited extinction ratio or from the presence of detrimental temporal sidelobes, so that a considerable part of the energy lies outside the main pulses [7]. In order to reject these residual background and tails, various architectures have been proposed, such as the use of a broadband optical carrier [8], of a nonlinear optical loop mirror [9] or of an additional amplitude modulation with optical bandpass spectral filtering [10].

*christophe.finot@u-bourgogne.fr; phone 33 380395926; fax 33 380395971

We introduce here theoretically and experimentally an alternative scheme where the quadratic spectral phase is replaced by a triangular one or by a set of discrete spectral phase shifts of π/2. After having detailed the theoretical basis of our approach, we present numerical simulations that demonstrate that with such a specific phase processing, Fourier-transform limited structures are obtained. We also discuss how it is possible to handle a dual tone sinusoidal phase modulation. Experimental validation based on standard components of the telecommunication industry has been carried out at repetition rates between 10 and 40 GHz. The results confirm that high-quality pulse trains can be achieved with an excellent extinction ratio. When the amplitude of the phase modulation is 1.1 rad, the pulses are close-to-Gaussian and with a duty cycle below 1/4, in full agreement with our numerical simulations and analytical predictions. We also stress that the resulting pulses may present some similarities with Akhmediev breathers at the point of maximum focusing. Finally, we experimentally show that proposed approach can be extended to process several wavelengths simultaneously as demonstrated by the experimental generation of 4 pulse trains at 40 GHz spaced by 400 GHz in the conventional C-band.

2. PRINCIPLE OF OPERATION

2.1 Our approach versus conventional method

In order to illustrate our approach, let us first consider a continuous optical wave ψ_0 which phase is temporally modulated by a sinusoidal waveform (for simplicity, the central optical carrier is here omitted):

$$\psi(t) = \psi_0 \, e^{i\,A\cos(2\pi f\,t)}, \tag{1}$$

where A is the amplitude of the phase modulation and f its frequency. We have plotted on Fig. 1(b-c) the resulting phase and intensity profiles both in the temporal and spectral domains for A = 1.1 rad. The temporal sinusoidal phase leads to a set of spectral lines that are equally spaced by f and which amplitude can be derived using a Jacobi-Anger expansion [11, 12]:

$$\psi(t) = \psi_0 \sum_{n=-\infty}^{\infty} i^n \, J_n(A) \, e^{i\,2\pi\,n\,f\,t} \tag{2}$$

Therefore, the n^{th} spectral component has an intensity proportional to J_n^2, with J_n being the Bessel function of the first kind of order n. An essential point that has not been stressed and exploited in the previous works is the existence of a phase shift of π/2 between each spectral component (Fig. 1(c1), cyan curve). Involving a dispersive effect, i.e. applying a quadratic spectral phase, cannot fully compensate for this phase profile (Fig. 1(c1), red curve). The residual phase leads to a deleterious background and a poor extinction ratio (panel b, red curve). With the progress of linear shaping, it has become now feasible to exactly compensate for the initial spectral phase profile (Fig. 1(c1), black curve). Therefore, a flat spectral phase can be achieved, leading to a Fourier-transform limited waveform that can be expressed as:

$$\psi'(t) = \psi_0 \left(J_0(A) + 2\sum_{n=1}^{\infty} J_n(A) \, \cos\left(2\pi \, n \, f \, t\right) \right) \tag{3}$$

As a consequence, in the temporal domain, the initial continuous wave is strongly reshaped into a train of well-separated ultrashort pulses at the repetition rate f (Fig. 1(b2,b3)). The extinction ratio is well above 20 dB and is clearly enhanced compared to the waveform resulting from a quadratic spectral phase. The full-width at half maximum (fwhm) duration is only ¼ of the period of the train and the pulse shape is very close from a Fourier-transform limited pulse.

However, as can be seen on panels (a) of Fig. 1, the quality of the generated pattern strongly depends on the phase modulation amplitude A on the resulting waveform. Higher A is, shorter are the generated pulses with an increased peak power. However, the extinction ratio of the pulse train does not evolve monotonously and a value around A = 1.1 rad leads to the lowest level of residual background.

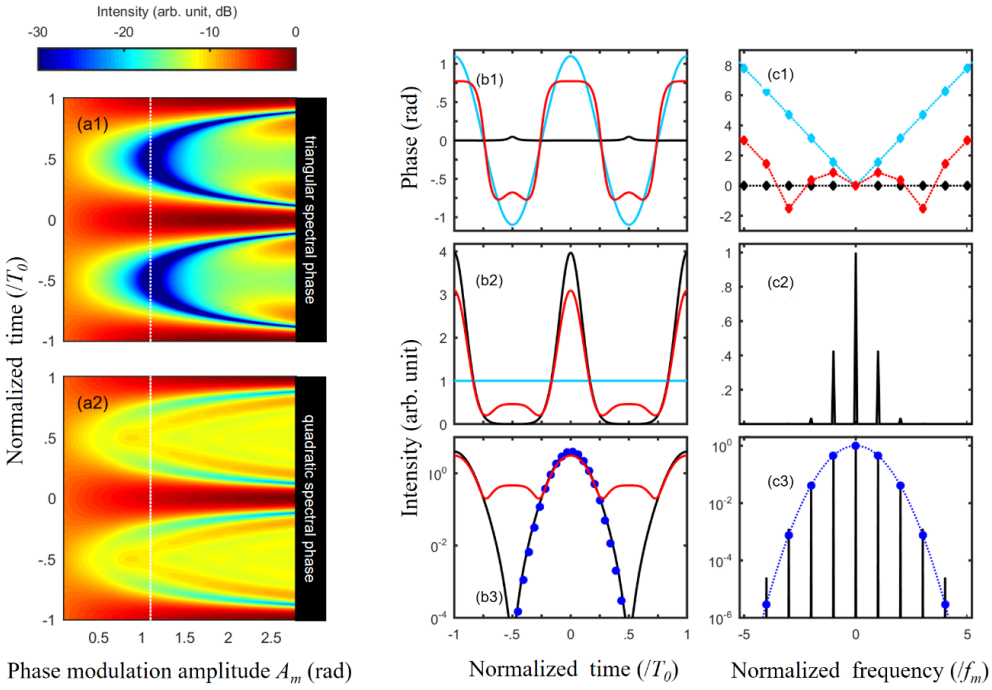

Figure 1. (a) Evolution of the temporal intensity profile according to the sinusoidal phase modulation amplitude *A*. Results of numerical simulations for a triangular or quadratic spectral phase compensation (panel a1 and a2, respectively). (b) Theoretical temporal and (c) spectral profiles predicted by A = 1.1 rad. Properties of the waveform after temporal phase modulation (cyan line) are compared with the results after spectral shaping with a triangular phase (black line), or with a quadratic phase (red line, the level of quadratic phase being chosen so as to optimize the peak power). The blue full circles correspond to a fit by a Fourier transform Gaussian pulse.

2.2 Pulse train resulting from a dual-tone phase modulation

Our method can be extended to generate a pulse train with properties varying from pulse-to-pulse. We replace the sinusoidal phase modulation used in (1) by a two-tone temporal phase modulation:

$$\varphi'(t) = A_1 \cos(2\pi\ f_1\ t) + A_2 \cos(2\pi\ f_2\ t)\,, \tag{4}$$

where A_1 and A_2 are the amplitude of the sinusoidal phase modulation at frequencies f_1 and $f_2 = f_1+\Delta f$, respectively. Combining these two sinusoidal modulations induces a beating characterized by fast oscillations with a frequency f' (leading to a period $T_0^{'}$) and by a slow envelope with a frequency f_b (leading to a period T_b). Typical examples of these temporal beatings are plotted on Fig. 2(a). Over the time scale of a fast temporal oscillation $T_0^{'}$, the phase-to-intensity conversion can be qualitatively as efficient as the one obtained based on a purely sinusoidal modulation with an amplitude $A^{'}$ provided by the envelope of the beating:

$$A^{'}(t) = \sqrt{A_1^2 + A_2^2 + 2\,A_1\ A_2 \cos(2\pi\,\Delta f\ t)}\,. \tag{5}$$

When $A_1 \gg A_2$ (see for example panel a1 of Fig. 2), the envelope of the phase modulation can be approximated by a sinusoidal modulation (black mixed line):

$$A^{'}(t) \simeq A_1 + A_2 \cos(\Delta\omega\, t)\,. \tag{6}$$

When A_1 = 1.1 rad, the peak-power of the resulting pulses is impacted by the beating and will also follow a sinusoidal variation (see Fig. 2(b1), black mixed line), which amplitude is directly controlled by A_2. Pulse duration also changes,

but for moderate values of A_2, the overall shape remains close to Gaussian. Another interesting case is when $A_1 = A_2$ (see Fig. 2(a2)). In this well-known case in wave physics [13], Eq. (5) can be rewritten as :

$$A'(t) \simeq 2A_1 \left|\cos(2\pi \Delta f\ t)\right| \tag{7}$$

The fast oscillations have a frequency $f' = \left(f_1 + f_2\right)/2$. The envelope is modulated between 0 and 2 A_1 at a frequency Δf. This results in rapidly varying pulses, with amplitude, duration, shape and extinction ratio experiencing major changes (see. Fig. 2(b2)).

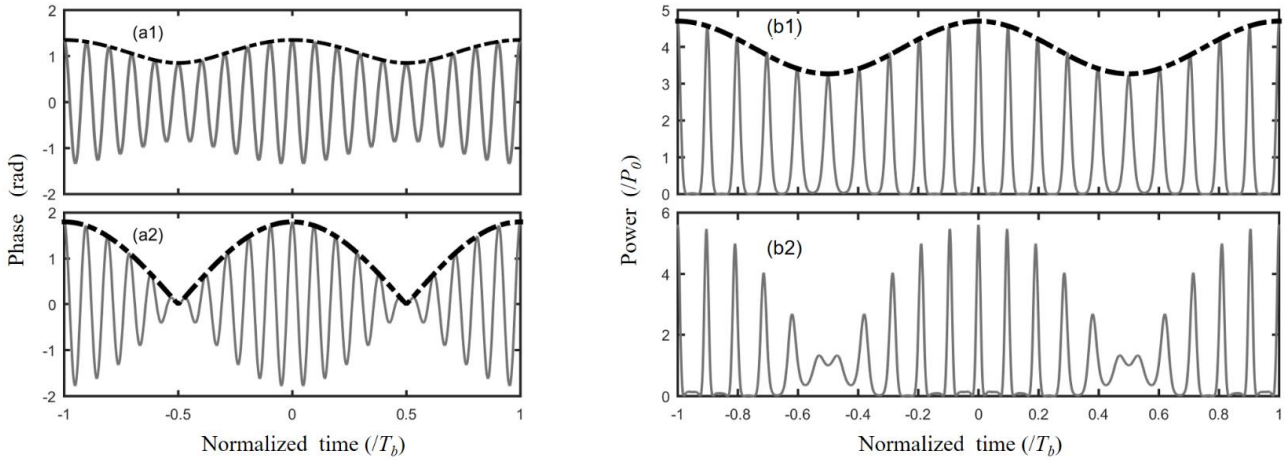

Figure 2. (a) Temporal phase profile resulting from the superposition of two sinusoidal phase modulation. (b) Resulting temporal intensity profiles after triangular spectral phase processing. Numerical results (grey line) are obtained at $\Delta f = 0.1\ f_1$ for $A_1 = 1.1$ rad and $A_2 = 0.25$ rad (panels 1) or for $A_1 = .9$ rad and $A_2 = .9$ rad (panels 2). Black mixed line represents the evolutions of the envelopes that can be theoretically predicted.

3. EXPERIMENTAL IMPLEMENTATION

The experimental setup we implement is sketched in Fig. 3 and is based on devices that are commercially available and typical of the telecommunication industry. In order to validate the principle of our approach, we use a continuous wave laser emitting in the conventional band of optical communications, i.e. around 1550 nm. The mW-wave is phase modulated using a Lithium Niobate modulator driven by an amplified sinusoidal electrical signal with f = 14 GHz, 20 GHz or 40 GHz. A linear spectral shaper (Finisar Waveshaper) based on liquid crystal on silicon technology [14, 15] is then used to apply the suitable equally spaced spectral $\pi/2$ phase shifts. Note that the discrete spectral phase profile can also be described by a triangular spectral phase profile. For operation at a fixed wavelength and a fixed repetition rate, the linear shaping stage can be fully realized by a cascaded uniform fiber Bragg grating [16]. In order to ensure enhanced environmental stability, polarization-maintaining components have been used.

The resulting signal is characterized with a high-resolution optical spectrum analyzer (5 MHz of resolution). The temporal aspects are monitored by means of a high-speed optical sampling oscilloscope (1 ps resolution) or by means of an electrical sampling oscilloscope (50 GHz bandwidth) connected to a high-speed photodiode (50 GHz bandwidth) and synchronized with the clock.

We also tested the ability of our proposed architecture to simultaneously deal with several channels at repetition rates f of 14 GHz or 40 GHz and with an amplitude A = 1.1 and 1 rad, respectively. An array of four continuous wave lasers with wavelengths spaced by 200 GHz or 400 GHz ((ranging from 1545.7 nm up to λ = 1551 nm or from λ = 1541.5 nm up to λ = 1551 nm) are wavelength multiplexed using a 200 GHz WDM multiplexers. By taking into account an additional linear spectral phase, the component can also be used to control accurately the delay of each channel. Moreover, the equipment can also accommodate the various power levels delivered by the continuous wave lasers. The records may be

obtained after wavelength demultiplexing using a dedicated component or using directly the wavelength routing ability of the spectral shaper.

Finally, in order to test the dual-tone modulation, the continuous wave at 1550 nm is then temporally phase modulated using two Lithium Niobate electro-optic devices driven by sinusoidal electrical signals at frequencies f_1 = 10 GHz and f_2. The optical phase modulations have an amplitude A_1 and A_2. Note that a single phase modulator could be used if the electrical sinusoidal waveforms can be mixed in the electrical domain or if an arbitrary waveform generator is available.

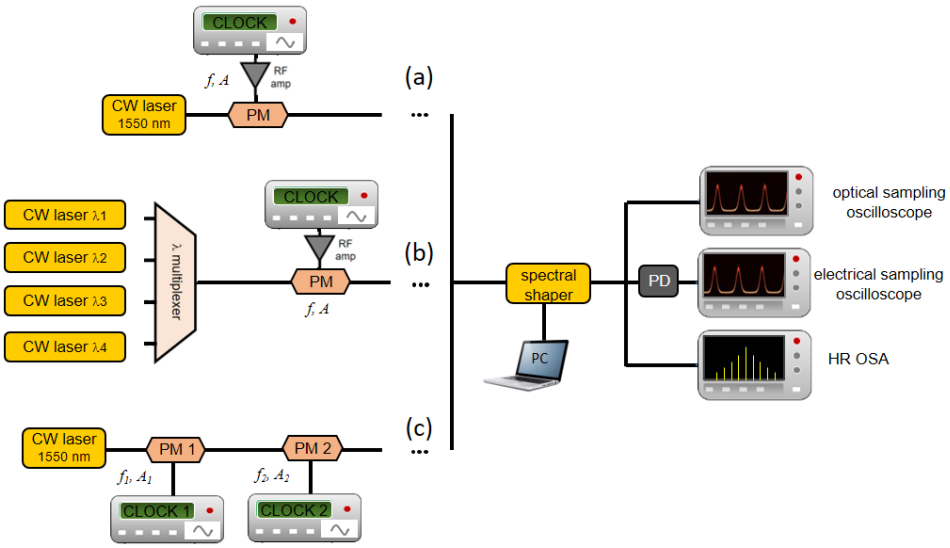

Figure 3. Experimental setups: CW : Continuous Wave; PM : Phase Modulator; PD : Photodiodes; HR OSA : High Resolution Optical Spectrum Analyzer. (a) Proof-of-principle experiment. (b) Multiwavelength operation. (c) Dual tone temporal phase modulation.

4. EXPERIMENTAL RESULTS

4.1 High quality pulse train generation

Experimental validation of high-quality pulse train generation is summarized in Fig. 4 for a repetition rate of 20 GHz and an amplitude of modulation of 1.1 rad that corresponds the optimum value predicted by the theoretical analysis. Pulses with an excellent extinction ratio (>20 dB) are recorded with a FWHM temporal duration of 12 ps in line with the numerical predictions. Figure 4(a) stresses the high level of stability of the pulse train with negligible temporal or amplitude jitter. The temporal intensity profile of the pulse can be closely approximated by a Gaussian waveform (Fig. 4(b)) and its spectrum corresponds to the Fourier transform limit (dotted blue line). High-resolution optical spectra (Fig. 4(c)) outline the quality of the resulting signal with an optical signal to noise ratio above 60 dB. Finally, we have also tested the capacity of our experimental setup to generate higher-repetition-rate pulse trains. Temporal intensity profiles obtained for f = 40 GHz are plotted in Figs. 4(d) on a linear and logarithmic scale. Temporal duration of 6.8 ps has been recorded, leading to duty cycles of 0.27. Results plotted on a logarithmic scale [Figs. 4(d2)] outline that the floor level is close to −20 dB (limited by the measurement capabilities of our temporal detection). Once again, the temporal intensity profiles exhibit an excellent pulse quality: no sidelobes are observed, and the profiles are closely adjusted by a Gaussian waveform.

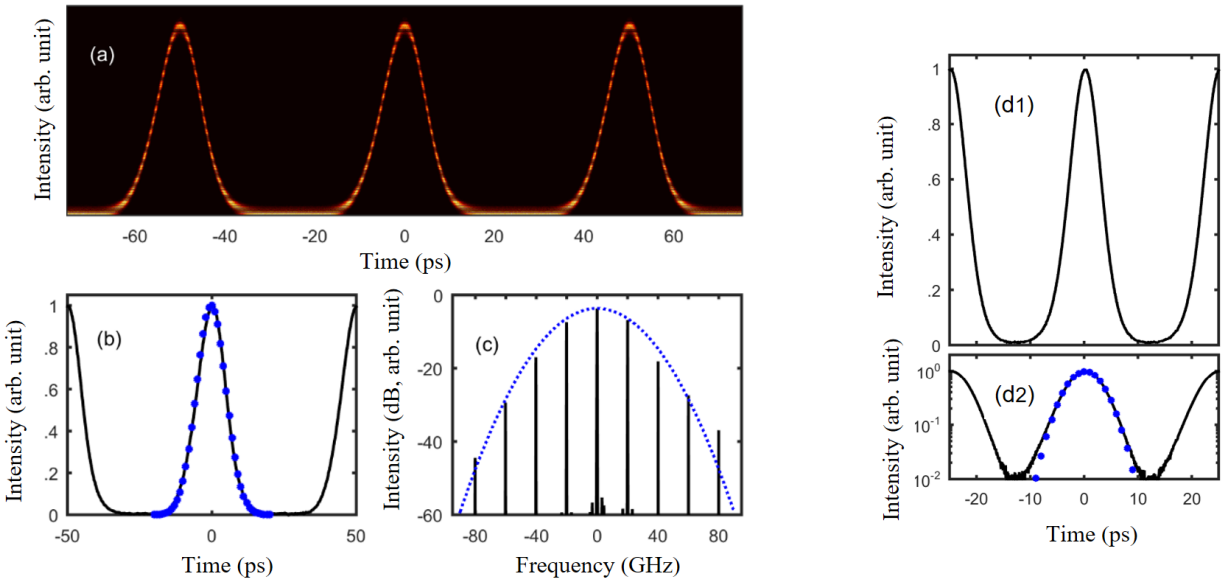

Figure 4. (a-c) Pulse properties achieved for A = 1.1 rad and a repetition rate f = 20 GHz. (a) Pulse train recorded in persistent mode on the optical sampling oscilloscope. (b) Temporal and (c) spectral intensity profiles (solid black lines). (d) Experimental results obtained at f =40 GHz and A = 1 rad. The results are displayed on a linear and logarithmic scale (panels 1 and 2). The experimental results are compared to a fit by a Fourier transform-limited Gaussian waveform (blue circles or blue dotted line).

4.2 Temporal waveform and breathers

Details of temporal measurements carried out at f = 20 GHz and for other values of A (0.5, 1 and 1.4 rad) are reported in Fig. 5(a). It is quite interesting to note the excellent agreement between theses profiles resulting from the phase modulation of a continuous wave and the analytical profiles of breathers that is expressed at the point of maximum compression in normalized units by [17]:

$$\psi_B(t) = \sqrt{P_0}\,\frac{(1-4a)+\sqrt{2a}\cos(2\pi\ f\ t)}{\sqrt{2a}\cos(2\pi\ f\ t)-1} \tag{8}$$

with $2a = 1-(2\pi\ f\ /\ \omega_c)^2$ and $\omega_c^2 = 4\gamma P_0\ /\ |\beta_2|$, P_0 being the average power of the wave, γ and β_2 the nonlinear and group velocity dispersion coefficients respectively of the nonlinear propagation.

Breathers are intrinsically nonlinear structures that are solutions of the nonlinear Schrödinger equation and that have been extensively investigated in recent years in fibers in the context of modulation instability, optical rogue waves [18, 19] and optical high-repetition sources [20, 21]. The optical spectra shown in Fig. 5(b) further confirm the similarity observed in the frequency domain with an excellent agreement over several orders of magnitude. Here, we therefore show that a simple and cost-efficient alternative based on electrooptic phase modulation yields AB-like structures with low a in the vicinity of the point of maximum compression.

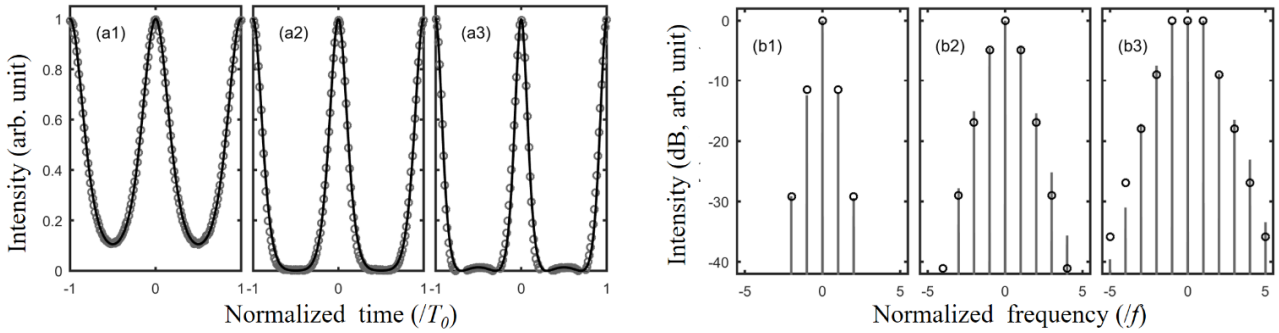

Figure 5. Temporal and spectral intensity profiles (panels a and b, respectively). Experimental records obtained for phase modulation A of 0.5, 1 and 1.41 rad (grey circles or line ; panels 1, 2 and 3, respectively) are compared with the analytical profiles of a AB with a parameters of 0.032, 0.11 and 0.2 (black line or circles).

4.3 Multiwavelength operation

Results of multiwavelength processing are summarized in Fig. 6 for operation with 4 channels at repetition rates of 14 and 40 GHz. Regarding the spectral aspects (Fig. 6a and c), we do not observe any sign of crosstalk between the different channels. Each pulse train exhibit a similar spectral waveform that can be fitted by a Gaussian shape. The temporal results are reported on panels b and d and confirm the absence of interferences between the various channels that are not affected by the presence of neighboring channels. For both repetition rates, the time-bandwidth products that are measured are close to 0.45 suggesting once again that the pulses are Fourier-transform limited waveforms.

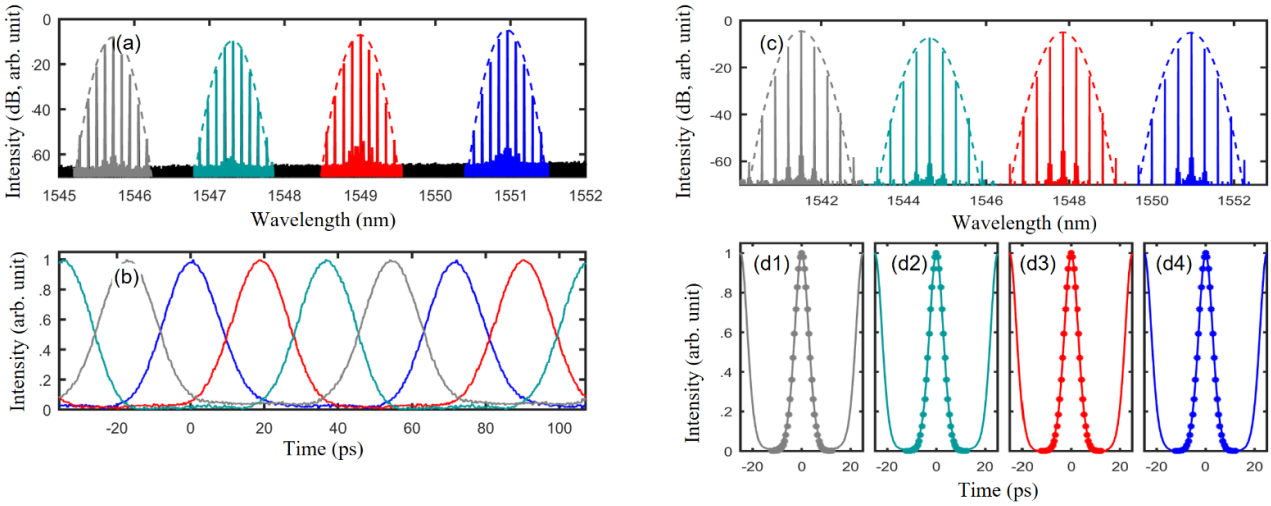

Figure 6. Experimental results obtained for a repetition rate of (a-b) 14 GHz with channels spaced by 200 GHz or (c-d) 40 GHz with channels spaced by 400 GHz. (a,c) Optical spectrum. Dashed lines are fits by a Gaussian waveform. (b, d) Temporal intensity profile of the various channels. [(b) Each channel is recorded on the electrical sampling oscilloscope after wavelength demultiplexing; (d) Each channel is recorded on the optical sampling oscilloscope after wavelength demultiplexing. The blue circles represent a fit by a Gaussian waveform.]

4.4 Temporal beating

In order to validate the operation using a dual tone phase modulation, we have first recorded the temporal waveforms that are generated when temporal phase modulations have frequencies of f_1 = 10 GHz and f_2 = 11 GHz, associated with an amplitude of modulation of A_1 = 1.1 rad and A_2 = 0.25 rad (panel a of Fig. 7) or A_1 = A_2 = 0.9 rad (panel b of Fig. 7).

The experimental waveforms outline that modification of the temporal pulse properties on a pulse-to-pulse basis is efficiently achieved: in both cases, each pulse of the 10 pulses sequence exhibits features that are different from its nearest neighbor. Changes in the peak-power are associated with changes of the temporal duration and the residual background can also vary. The excellent agreement that is obtained with the numerical simulations (see dotted grey line) stresses the accurate control that can be achieved by simply adjusting the amplitude of the phase modulation.

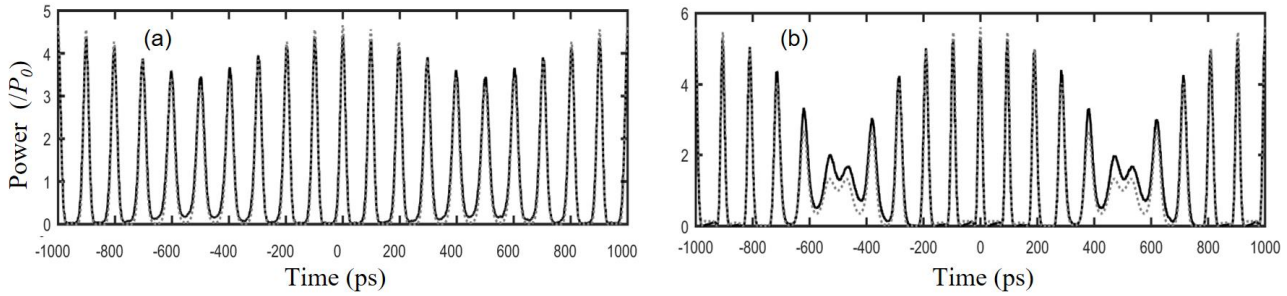

Figure 7. Temporal intensity profiles resulting from the superposition of two sinusoidal phase modulation and spectral processing. Results obtained for A_1 = 1.1 rad and A_2 = 0.25 rad (panel a1) or for A_1 = .9 rad and A_2 = .9 rad (panel a2). Experimental results recorded on the optical sampling oscilloscope (solid black line) are compared with numerical simulations (grey dotted lines)

5. CONCLUSIONS

We have introduced theoretically and validated experimentally an alternative scheme where a sinusoidal modulation of the temporal phase can be efficiently converted into a train of well-defined optical pulses at repetitions rates between 10 and 40 GHz [22]. Fourier-transform limited structures are obtained, with properties that may present some similarities with Akhmediev breathers at the point of maximum focusing [23]. The experimental results have confirmed the excellent extinction ratio that can be achieved. When the amplitude of the phase modulation is 1.1 rad, the pulses are close-to-Gaussian and with a duty cycle below 1/4, in full agreement with our numerical simulations and analytical predictions. Higher compression ratio can be reached and pulses of a few picoseconds can be generated at 20 GHz, but this is at the expense of some temporal sidelobes. The reshaping process is here quite energy efficient, since the optical losses are restricted to the insertion losses of the phase modulator and of the spectral shaper. Moreover, since the principle of operation is purely linear, no erbium-doped fiber amplifier is required, thus limiting the source of detrimental noise. Moreover, in contrast to nonlinear reshaping schemes that may suffer from severe Brillouin backscattering in fiber segments under test, it is not here required to involve additional phase modulation that may turn into unwanted intensity fluctuations [24]. Consequently, the resulting pulse train exhibits remarkable stability.

The proposed approach has been extended to process several wavelengths simultaneously as demonstrated by the experimental generation of 4 pulse trains at 40 GHz spaced by 400 GHz in the conventional C-band [25, 26]. The versatility of this all-optical scheme also enables the generation of pulse trains with varying pulse-to-pulse delays or durations. Indeed, we show that this technic relying on discrete spectral phase shifts can fully sustain a temporal phase modulation with a linear frequency chirp [27] as well as a dual-tone temporal phase modulation [28]. The experimental demonstration has been achieved at 1550 nm, but the method can be straightforwardly adapted to any other wavelength where high-speed phase modulators are available.

ACKNOWLEDGEMENT

We acknowledge the support of the Institut Universitaire de France (IUF), the Bourgogne-Franche Comté Region, the French Investissements d'Avenir program and the Agence Nationale de la Recherche (ANR-11-LABX-01-01). We thank Julien Fatome, Bertrand Kibler, Kamal Hammani and John M. Dudley for fruitful discussions or technical help. The article has benefited from the PICASSO experimental platform of the University of Burgundy.

REFERENCES

[1] T. Inoue, and S. Namiki, "Pulse compression techniques using highly nonlinear fibers," Laser Photonics Rev., 2(1), 83-99 (2008).

[2] S. Pitois, C. Finot, J. Fatome *et al.*, "Generation of 20-Ghz picosecond pulse trains in the normal and anomalous dispersion regimes of optical fibers," Opt. Commun., 260(1), 301-306 (2006).

[3] C. Finot, J. Fatome, S. Pitois *et al.*, "All-Fibered High-Quality Low Duty-Cycle 20-GHz and 40-GHz Picosecond Pulse Sources," IEEE Photon. Technol. Lett., 19(21), 1711-1713 (2007).

[4] T. Kobayashi, H. Yao, K. Amano *et al.*, "Optical pulse compression using high-frequency electrooptic phase modulation," IEEE J. Quantum Electron., 24(2), 382-387 (1988).

[5] T. Komukai, Y. Yamamoto, and S. Kawanishi, "Optical pulse generator using phase modulator and linearly chirped fiber Bragg gratings," IEEE Photon. Technol. Lett., 17(8), 1746-1748 (2005).

[6] J. Nuno, C. Finot, and J. Fatome, "Linear Sampling and Magnification Technique Based on Phase Modulators and Dispersive Elements: the Temporal Lenticular Lens," Opt. Fiber Technol., 36, 125-129 (2017).

[7] V. Torres-Company, J. Lancis, and P. Andrés, "Unified approach to describe optical pulse generation by propagation of periodically phase-modulated CW laser light," Opt. Express, 14(8), 3171-3180 (2006).

[8] J. Lancis, V. Torres-Company, P. Andres *et al.*, "Side-lobe suppression in electro-optic pulse generation," Electron. Lett., 43(7), 414-415 (2007).

[9] S. Yang, and X. Bao, "Generating a high-extinction-ratio pulse from a phase-modulated optical signal with a dispersion-imbalanced nonlinear loop mirror," Opt. Lett, 31(8), 1032-1034 (2006).

[10] H. Hu, J. Yu, L. Zhang *et al.*, "Pulse source based on directly modulated laser and phase modulator," Opt. Express, 15(14), 8931-8937 (2007).

[11] K. Hammani, J. Fatome, and C. Finot, "Applications of sinusoidal phase modulation in temporal optics to highlight some properties of the Fourier transform," Eur. J. Phys., 40, 055301 (2019).

[12] C. Finot, F. Chaussard, and S. Boscolo, "Impact of a temporal sinusoidal phase modulation on the optical spectrum," Eur. J. Phys., 39, 055303 (2018).

[13] F. Crawford, "Waves : Berkeley Physics Course Volume 3."

[14] M. A. F. Roelens, S. Frisken, J. Bolger *et al.*, "Dispersion trimming in a reconfigurable wavelength selective switch," J. Lightw. Technol., 26, 73-78 (2008).

[15] Z. Jiang, D. E. Leaird, and A. M. Weiner, "Optical processing based on spectral line-by-line pulse shaping on a phase-modulated CW laser," IEEE J. Quantum Electron., 42(7), 657-665 (2006).

[16] N. K. Berger, B. Levit, and B. Fischer, "Reshaping periodic light pulses using cascaded uniform fiber Bragg gratings," J. Lightw. Technol., 24(7), 2746-2751 (2006).

[17] N. N. Akhmediev, and V. I. Korneev, "Modulation instability and periodic-solutions of the nonlinear Schrödinger equation," Theor. Math. Phys., 69(2), 1089-1093 (1986).

[18] J. M. Dudley, F. Dias, M. Erkintalo *et al.*, "Instabilities, breathers and rogue waves in optics," Nat. Photon., 8(10), 755-764 (2014).

[19] F. Copie, S. Randoux, and P. Suret, "The Physics of the one-dimensional nonlinear Schrödinger equation in fiber optics: Rogue waves, modulation instability and self-focusing phenomena," Reviews in Physics, 5, 100037 (2020).

[20] B. Varlot, Y. K. Chembo, and C. Finot, "Akhmediev breathers as ultra-wideband pulses," Microw. Opt. Technol. Lett., 56, 664–667 (2014).

[21] J. Fatome, B. Kibler, and C. Finot, "High-quality optical pulse train generator based on solitons on finite background," Opt. Lett., 38(10), 1663-1665 (2013).

[22] U. Andral, J. Fatome, B. Kibler *et al.*, "Triangular spectral phase tailoring for the generation of high-quality picosecond pulse trains," Opt. Lett., 44(19), 4913 (2019).

[23] U. Andral, B. Kibler, J. M. Dudley *et al.*, "Akhmediev breather signatures from dispersive propagation of a periodically phase-modulated continuous wave," submitted, arXiv:1907.08426.

[24] I. El Mansouri, J. Fatome, C. Finot *et al.*, "All-Fibered High-Quality Stable 20- and 40-GHz Picosecond Pulse Generators for 160-Gb/s OTDM Applications," IEEE Photon. Technol. Lett., 23(20), 1487-1489 (2011).

[25] J. van Howe, J. Hansryd, and C. Xu, “Multiwavelength pulse generator using time-lens compression,” Opt. Lett., 29(13), 1470-1472 (2004).
[26] U. Andral, and C. Finot, “Multiwavelength high-repetition rate source,” Laser Phys., 30, 016203 (2020).
[27] C. Finot, “Frequency-swept high-repetition rate optical source,” submitted, preprint arXiv:2001.04262.
[28] U. Andral, and C. Finot, “High-repetition-rate source delivering optical pulse trains with a controllable level of amplitude and temporal jitters,” submitted, arXiv:1910.11739.